# Monometallic lanthanide complexes with tridentate 2,6-dicarboxamido-pyridine ligands. Influence of peripheral substitutions on steric congestion and antenna effect

---

Thierry Le Borgne, Jean-Marc Bénech, Sébastien Floquet, Gérald Bernardinelli, Christian Aliprandini, Philippe Bettens, and Claude Piguet *

## Supporting Information

Table S1 Selected $^1$H NMR chemical shifts (δ /ppm *vs* TMS) for the ligands **L5**-**L8** ($d^6$-DMSO, 298 K).

| Ligand | H1 | H2 | H5 | H6 | H7 | H8 | H9 | H10 |
|---|---|---|---|---|---|---|---|---|
| **L5**[a] | 7.87 | 7.63 | 3.56 | 1.26 | - | 3.34 | 1.15 | - |
| **L6** | 7.91 | 7.39 | 3.56 | 1.39 | 1.39 | 3.54 | 1.05 | 1.05 |
| **L7** | 8.23 | 8.12 | 4.56 | - | - | - | - | - |
| **L8** | 8.00 | 7.69 | 4.49 | 4.26 | - | - | - | - |

[a] Taken from ref. 19 in $CD_3CN$.

Table S2 Elemental analyses for the complexes $[Ln(\mathbf{L6})_2](CF_3SO_3)_3{\cdot}xH_2O{\cdot}y$THF (Ln = Eu, $x$ = 2, $y$ = 0: **1**; Ln = Gd, $x = y = 0$: **2;** Ln = Tb, $x = y = 0$: **3;** Ln = Lu, $x = 0$, $y = 1.5$: **4**) and $[Ln(\mathbf{L7})_2](CF_3SO_3)_3{\cdot}xH_2O{\cdot}y$THF (Ln = Eu, $x = 1$, $y = 0$: **5**; Ln = Gd, $x = 0$, $y = 2$: **6;** Ln = Tb, $x = 3$, $y = 0$: **7;** Ln = Lu, $x = 1$, $y = 0$: **8**). Calculated values are given in parentheses.

| Compound | % C | % H | % N |
|---|---|---|---|
| $[Eu(\mathbf{L6})_2](CF_3SO_3)_3{\cdot}2H_2O$ (**1**) | 38.1 (38.05) | 4.8 (4.52) | 6.5 (6.49) |
| $[Gd(\mathbf{L6})_2](CF_3SO_3)_3$ (**2**) | 38.8 (38.73) | 5.0 (4.92) | 6.4 (6.61) |
| $[Tb(\mathbf{L6})_2](CF_3SO_3)_3$ (**3**) | 39.1 (38.68) | 5.2 (4.91) | 6.3 (6.60) |
| $[Lu(\mathbf{L6})_2](CF_3SO_3)_3{\cdot}1.5$THF (**4**) | 40.7 (40.40) | 5.4 (5.34) | 6.4 (6.01) |
| $[Eu(\mathbf{L7})_2](CF_3SO_3)_3{\cdot}H_2O$ (**5**) | 52.8 (52.55) | 4.1 (3.87) | 5.0 (5.04) |
| $[Gd(\mathbf{L7})_2](CF_3SO_3)_3{\cdot}2$THF (**6**) | 54.2 (54.1) | 4.5 (4.37) | 4.7 (4.67) |
| $[Tb(\mathbf{L7})_2](CF_3SO_3)_3{\cdot}3H_2O$ (**7**) | 51.0 (51.23) | 4.1 (4.00) | 4.7 (4.91) |
| $[Lu(\mathbf{L7})_2](CF_3SO_3)_3{\cdot}H_2O$ (**4**) | 52.1 (51.84) | 4.0 (3.81) | 4.9 (4.97) |

Table S3 Calculated distribution of isomers for $[Ln(\mathbf{L8})_3]^{3+}$ by using a statistical 1:2:1 distribution of the *EE*:*EZ*:ZZ conformers for each ligand strand.

| Isomers | Degeneracy | Distribution / % | Point group |
|---|---|---|---|
| $(EE)^3$ | 1 | 1.6 | $D_3$ |
| $(ZZ)^3$ | 1 | 1.6 | $D_3$ |
| $(EE)^2(ZZ)$ | 3 | 4.7 | $C_2$ |
| $(EE)(ZZ)^2$ | 3 | 4.7 | $C_2$ |
| $(EE)^2(EZ)$ | 6 | 9.3 | $C_1$ |
| Syn-$(EE)(EZ)^2$ | 6 | 9.3 | $C_2$ |
| Anti-$(EE)(EZ)^2$ | 6 | 9.8 | $C_1$ |
| $(ZZ)^2(EZ)$ | 6 | 9.3 | $C_1$ |
| Syn-$(ZZ)(EZ)^2$ | 6 | 9.3 | $C_2$ |
| Anti-$(ZZ)(EZ)^2$ | 6 | 9.3 | $C_1$ |
| $(EE)(ZZ)(EZ)$ | 12 | 18.8 | $C_1$ |
| Mer-$(EZ)^3$ | 6 | 9.3 | $C_1$ |
| Fac-$(EZ)^3$ | 2 | 3.2 | $C_3$ |

Table S4 Selected structural data for the lanthanide coordination spheres in $[Tb(\mathbf{L8})_3]_2(CF_3SO_3)_6(C_3H_5N)_3(H_2O)$ (**11**).

| Angles $\phi$ [a] / ° | | | |
|---|---|---|---|
| Compd | **11a** | **11b** | Perfect TTP[b] |
| $R^1$-Tb-$R^2$ | 178.1 | 178.9 | 180 |

| Angles $\theta_t$ [a] / ° (distal tripods) | | | | |
|---|---|---|---|---|
| Compd | **11a** | | **11b** | Perfect TTP[b] |
| $R^1$-Tb-O1b | 49.7 | $R^1$-Tb-O1d | 47.4 | $\alpha$ |
| $R^1$-Tb-O1a | 48.5 | $R^1$-Tb-O2e | 47.6 | $\alpha$ |
| $R^1$-Tb-O1c | 49.7 | $R^1$-Tb-O2f | 45.0 | $\alpha$ |
| $R^2$-Tb-O2a | 50.6 | $R^2$-Tb-O2d | 49.1 | $\alpha$ |
| $R^2$-Tb-O2b | 46.5 | $R^2$-Tb-O1e | 47.7 | $\alpha$ |
| $R^2$-Tb-O2c | 47.9 | $R^2$-Tb-O1f | 46.0 | $\alpha$ |

| Angles $\omega_{ij}$ [a] / ° | | | | |
|---|---|---|---|---|
| Compd | **11a** | | **11b** | Perfect TTP[b] |
| Proj[O1a]-Tb-Proj[O2b][c] | 12.4 | Proj[O1d]-Tb-Proj[O1f] | 13.6 | 0 |
| Proj[O1b]-Tb-Proj[O2c] | 9.6 | Proj[O2e]-Tb-Proj[O2d] | 15.5 | 0 |
| Proj[O2a]-Tb-Proj[O2c] | 10.8 | Proj[O1e]-Tb-Proj[O2f] | 13.0 | 0 |

[a] For the definition of $\phi$, $\theta_i$ and $\omega_{ij}$, see the associated scheme. The error in the angles is typically 0.5°. [b] TTP = tricapped trigonal prism. [c] Proj[O($i$)] and Proj[N($i$)] are the projections of O($i$) and respectively N($i$) along the $R^1$-$R^2$ direction onto a perpendicular plane passing through the lanthanide atom. $R^1$ = Tb-O1a + Tb-O1b + Tb-O1c and $R^2$ = Tb-O2a + Tb-O2b + Tb-O2c.

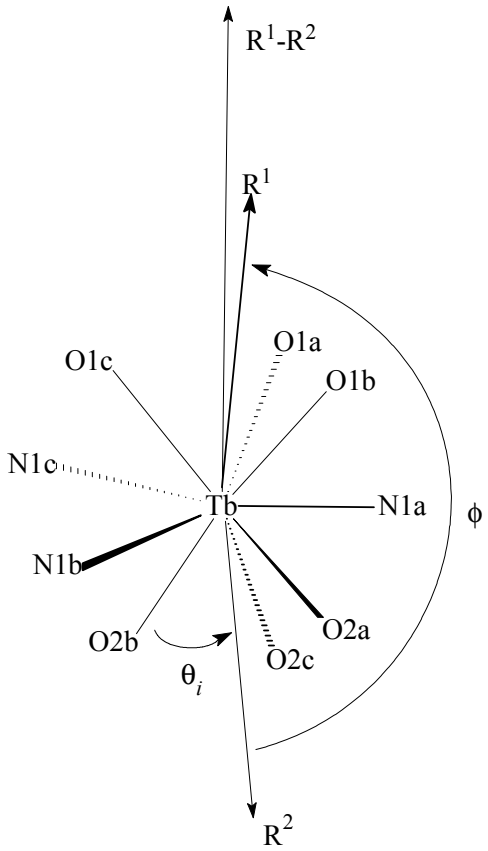
R1-R2
R1
O1a
O1c
O1b
N1c
Tb
N1a
ϕ
N1b
O2b
O2a
O2c
θi
R2

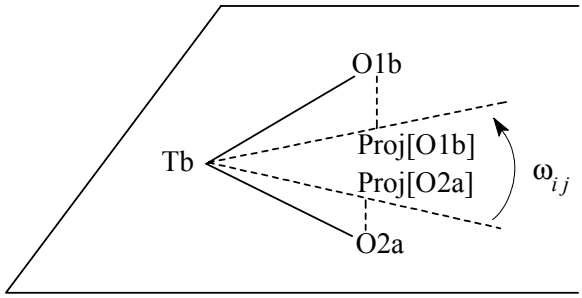
O1b
Tb
Proj[O1b]
Proj[O2a]
ωij
O2a

Table S5 Intra- and intermolecular stacking (S) and "edge to face" (T) interactions occurring in the crystals of $[Tb(\mathbf{L8})_3]_2(CF_3SO_3)_6(CH_3CH_2CN)_3(H_2O)$ (**11**, ϕ = benzyl, Py = pyridine)

| | Pya | ϕ1a | ϕ2a | Pyb | ϕ1b | ϕ2b | Pyc | ϕ1c | ϕ2c | Pyd | ϕ1d | ϕ2d | Pye | ϕ1e | ϕ2e | Pyf | ϕ1f | ϕ2f |
|---|---|---|---|---|---|---|---|---|---|---|---|---|---|---|---|---|---|---|
| Pya | | | | | | S | | S | | | | | | | | | | |
| ϕ1a | | | T [2] | S | | | | | | | | | | | | | | |
| ϕ2a | | T [2] | | | | | T | T | | | | | | | | | | |
| Pyb | | S | | | | | | | S | | | | | | | | | |
| ϕ1b | | | | | | | T | | T | | | | | | | | | |
| ϕ2b | S | | | | | | | | | | | | | | | | | |
| Pyc | | | T | | T | | | | | | | | | | | | | |
| ϕ1c | S | | T | | | | | | | S [1] | T [1] | | | | | | | |
| ϕ2c | | | | S | T | | | | | | | | S [3] | T [4] | | | | |
| Pyd | | | | | | | | S [1] | | | | | | | S | | | |
| ϕ1d | | | | | | | | T [1] | | | | | | | | T | | |
| ϕ2d | | | | | | | | | | | | | S | | | | | |
| Pye | | | | | | | | | S [3] | | | S | | | | | | |
| ϕ1e | | | | | | | | | T [4] | | | | | | | T | | |
| ϕ2e | | | | | | | | | | S | | | | T | | | | |
| Pyf | | | | | | | | | | | T | | | | | | | |
| ϕ1f | | | | | | | | | | | | | | | | | | |
| ϕ2f | | | | | | | | | | | | | | | | | | |

Intramolecular Intermolecular

[1] Between the two cations of the asymmetric unit. [2] Between x, y, z (ϕ2a) and 2-x, 3/2+y, -z (ϕ1a, interlayers). [3] Between x, y, z (ϕ2c) and x+1, y, z-1 (Pye, intralayer). [4] Between x, y, z (ϕ1e) and x-1, y, z+1 (ϕ2c, intralayer).

Table S6. Summary of crystal data, intensity measurement and structure refinement for **L8**, $[Eu(\mathbf{L6})_2(H_2O)_2(CF_3SO_3)]$ $(CF_3SO_3)_2(THF)_{1.5}$ (**9**), $[Gd(\mathbf{L7})_2(H_2O)_2(CF_3SO_3)](CF_3SO_3)_2(^tBuOMe)_2$ (**10**) and $[Tb(\mathbf{L8})_3]_2(CF_3SO_3)_6(CH_3CH_2CN)_3(H_2O)$ (**11**).

| | **L8** | **9** | **10** | **11** |
|---|---|---|---|---|
| Formula | $C_{21}H_{19}N_3O_2$ | $C_{47}H_{78}EuF_9N_6O_{16.5}S_3$ | $C_{83}H_{90}F_9GdN_6O_{17}S_3$ | $C_{141}H_{131}F_{18}N_{21}O_{31}S_6Tb_2$ |
| Mol. wt. | 345.4 | 1410.5 | 1868.2 | 3468.1 |
| Crystal Size (mm) | 0.13 x 0.21 x 0.29 | 0.08 x 0.10 x 0.38 | 0.09 x 0.17 x 0.33 | 0.08 x 0.28 x 0.33 |
| Crystal system | monoclinic | monoclinic | monoclinic | monoclinic |
| Space Group | *P* $2_1/c$ | *P* $2_1/c$ | *I* 2/*a* | *P* $2_1$ |
| a (Å) | 15.9562(12) | 14.6845(6) | 24.0530(11) | 16.0103(7) |
| b (Å) | 11.0886(8) | 25.3495(13) | 15.0320(6) | 28.0794(13) |
| c (Å) | 9.9212(7) | 18.3302(8) | 48.983(3) | 17.3614(7) |
| β (°) | 97.695(9) | 101.303(5) | 99.378(6) | 93.889(5) |
| V ($Å^3$) | 1739.6(2) | 6691.0(6) | 17473.8(15) | 7787.0(6) |
| Z | 4 | 4 | 8 | 2 (*Z'*=2) |
| $D_x$ gr.$cm^{-3}$ | 1.319 | 1.400 | 1.420 | 1.479 |
| μ(MoKα) $mm^{-1}$ | 0.087 | 1.118 | 0.917 | 1.080 |
| Tmin, Tmax | 0.9795 , 0.9893 | 0.8724 , 0.9210 | 0.8107 , 0.9176 | 0.7197 , 0.9181 |
| $((\sin\theta)/\lambda)_{max}$ ($Å^{-1}$) | 0.615 | 0.615 | 0.661 | 0.615 |
| No. measured reflc. | 18736 | 65007 | 116662 | 68845 |
| No. independent reflc. | 3365 | 12398 | 20939 | 30394 |
| No. observed reflc. | 1564 | 8091 | 11243 | 21740 |
| Criterion for observed | \|Fo\| > 4σ(Fo) | \|Fo\| > 4σ(Fo) | \|Fo\| > 4σ(Fo) | \|Fo\| > 4σ(Fo) |
| Refinement (on F) | Full-matrix | Full-matrix | Full-matrix | Full-matrix |
| No. parameters | 311 | 778 | 1157 | 1946 |
| Weighting scheme *p* [a] | 0.0002 | 0.0002 | 0.00015 | 0.0003 |
| Maximum Δ/σ | 0.002 | 0.002 | 0.18 | 0.009 |
| Max. and min. Δρ ($e.Å^{-3}$) | 0.23 , -0.19 | 0.89 , -0.66 | 0.94 , -1.39 | 0.87 , -0.66 |
| Flack parameter x | - | - | - | 0.069(12) |
| S [b] (all data) | 1.13 | 1.22 | 1.12 | 1.51 |
| R [c], ωR [d] | 0.031 , 0.031 | 0.033 , 0.035 | 0.037 , 0.037 | 0.041 , 0.042 |

a) $\omega = 1/[\sigma^2(F_o) + p(F_o)^2]$ ; b) $S = [\Sigma\{((F_o-F_c)/\sigma(F_o))^2\}/(N_{ref}-N_{var})]^{1/2}$

c) $R = \Sigma \, ||F_o| - |F_c|| \, / \, \Sigma \, |F_o|$ ; d) $\omega R = [\, \Sigma \, (\omega|Fo|-|Fc|)^2 \, / \, \Sigma \, \omega|Fo|^2]^{1/2}$

a)

b)

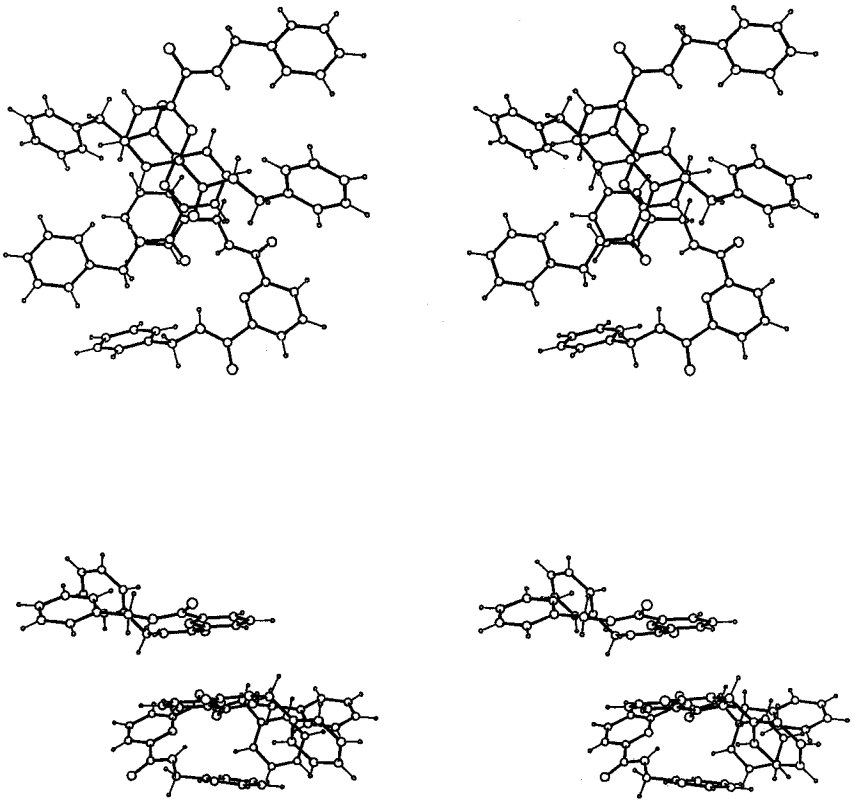

Figure S1 Stereoview of ligands **L8** in the crystal highlighting a) intermolecular hydrogen bonding (N2H02···O2' = 2.22(3) Å, N2-H02···O2' = 154(2)° and N3H03···O2' = 2.26(3) Å, N2-H02···O2' = 165(2)°, primed atoms correspond to x, ½-y, ½+z), and b) intermolecular offset face-to-face aromatic stacking interactions involving pyridine-pyridine pairs through a centre of inversion, and pyridine-benzyl pairs through a glide plane.

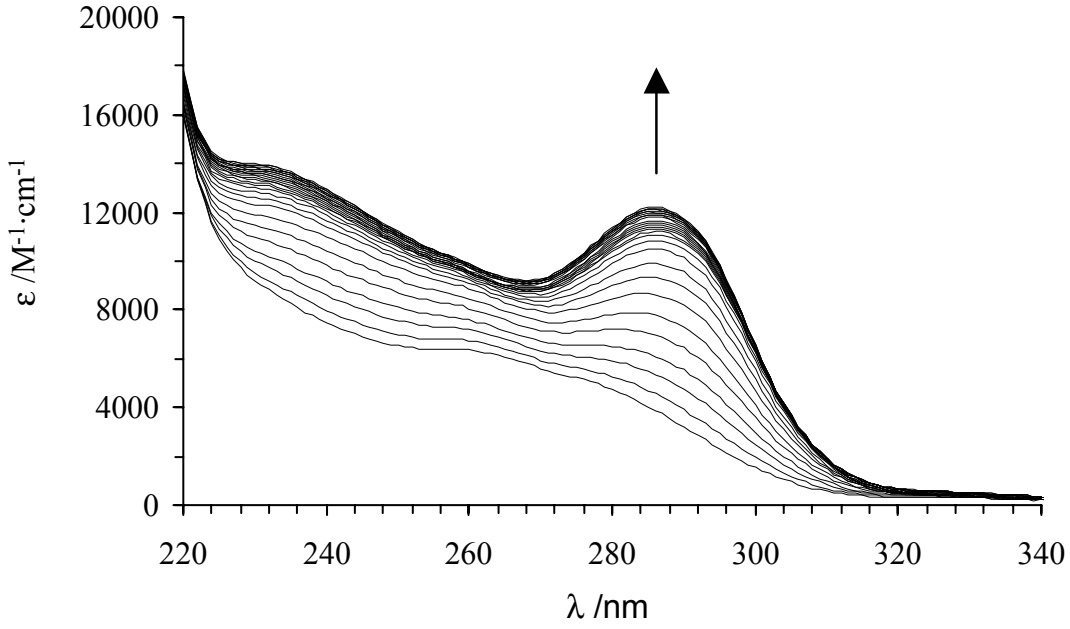


Figure S2 Variation of the absorption spectra observed for the spectrophotometric titration of **L7** ($10^{-4}$ mol·dm$^{-3}$ in acetonitrile) with $Lu(CF_3SO_3)_3 \cdot 2H_2O$ at 293 K (Lu:**L7** = 0.1-1.5).

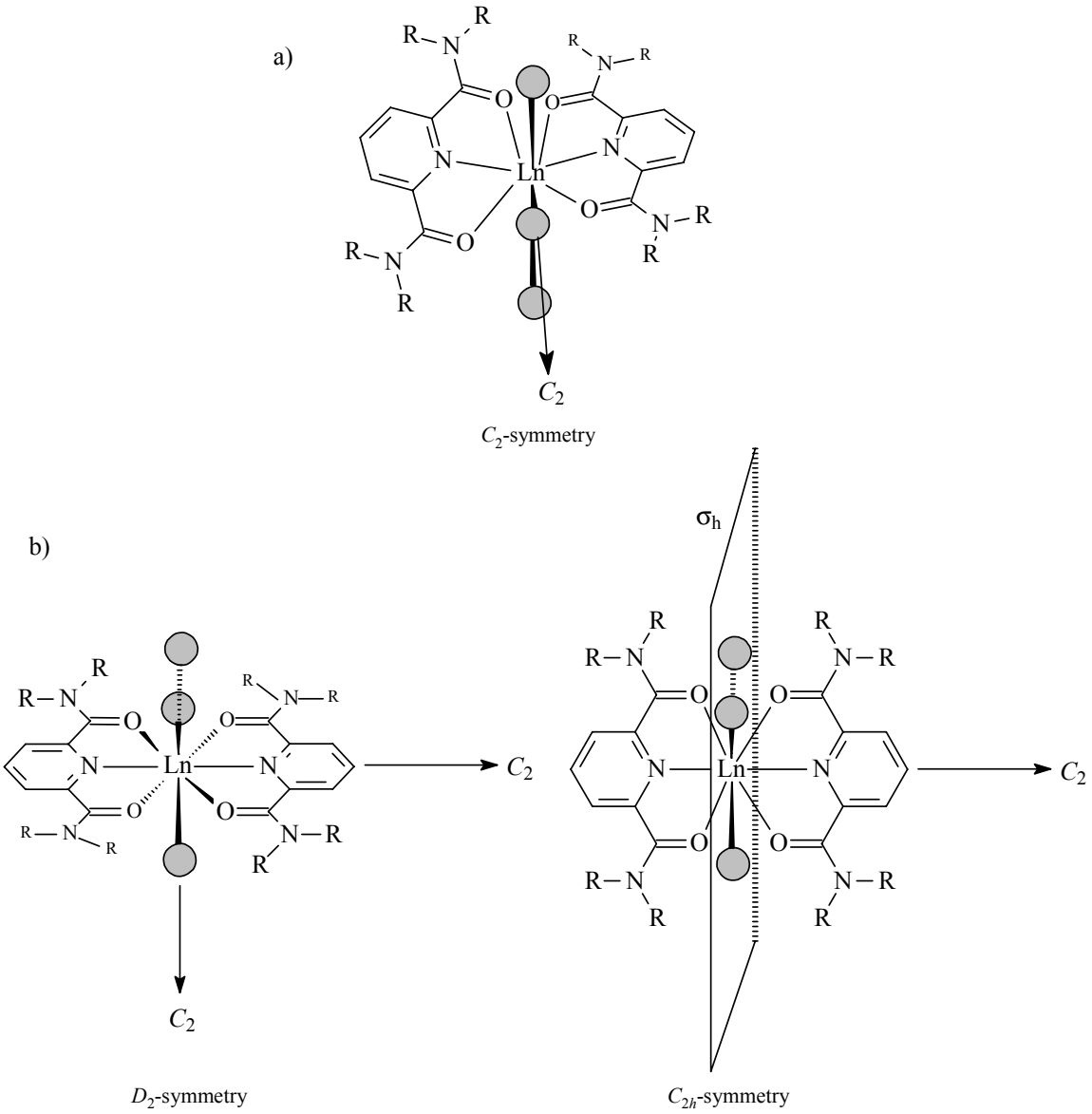


Figure S3 Dynamically-average structures observed in solution on the NMR time scale for a) $[Ln(\mathbf{L6})_2]^{2+}$ ($C_2$-symmetry: the twofold axis is located along the central Ln-solvent bond) and b) $[Ln(\mathbf{L7})_2]^{2+}$ ($D_2$-symmetry or $C_{2h}$-symmety: the solvent molecules (represented with grey spheres) occupy dynamically average positions within the meridional plane).

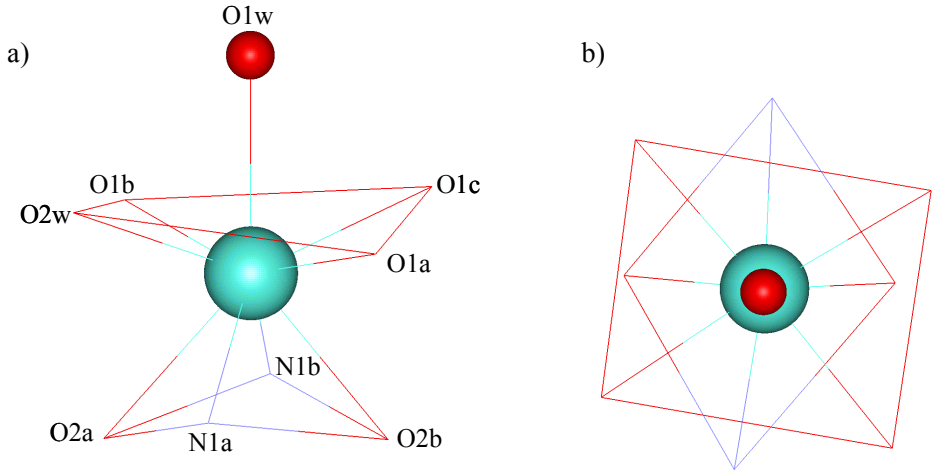


Figure S4 Perspective views of the co-ordination sphere in $[Gd(\mathbf{L7})_2(H_2O)_2(CF_3SO_3)]^{2+}$ a) perpendicular and b) along the Gd-O1w bond, thus highlighting the distorted monocapped square antiprismatic arrangements of the nine donor atoms.

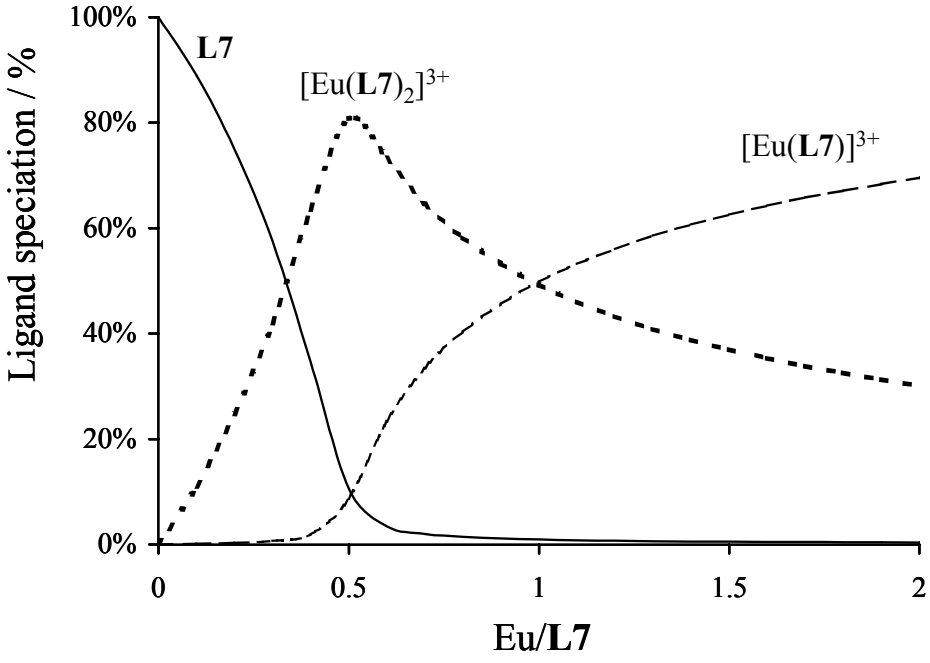


Figure S5 Distribution curves (ligand speciation) for the complexation of **L7** with $Eu(CF_3SO_3)_3{\cdot}2H_2O$ (acetonitrile, total ligand concentration: $2{\cdot}10^{-3}$ mol·dm$^{-3}$).

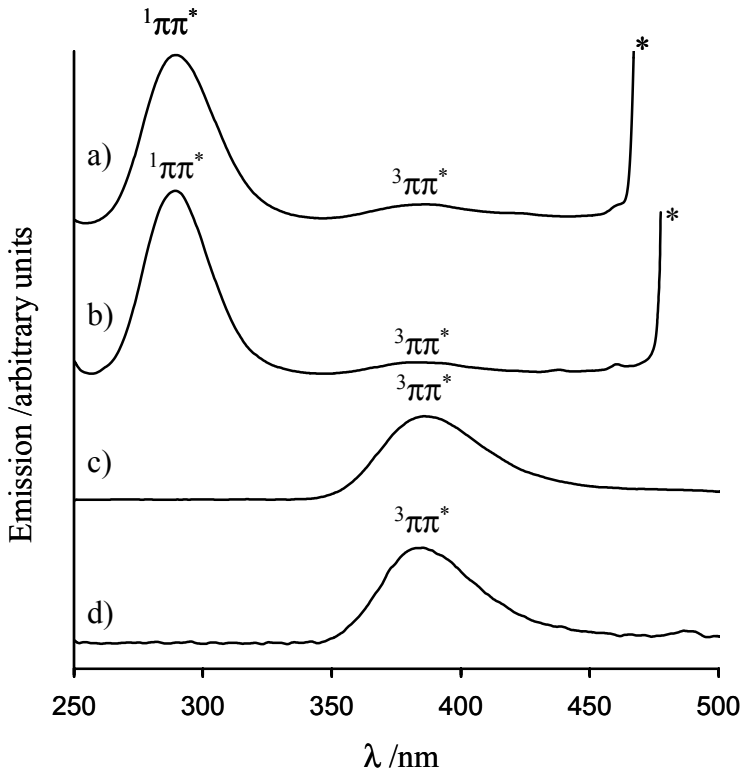


Figure S6 Fluorescence spectra of a) $[Gd(\mathbf{L6})_2](CF_3SO_3)_3$ (**2**, $\lambda_{exc}$ = 41665 $cm^{-1}$, 77K), b) $[Gd(\mathbf{L7})_2](CF_3SO_3)_3$ (**6**, $\lambda_{exc}$ = 41150 $cm^{-1}$, 77K), and time-resolved phosphorescence spectra (delay 0.1 ms) of c) $[Gd(\mathbf{L6})_2](CF_3SO_3)_3$ (**2**, $\lambda_{exc}$ = 41665 $cm^{-1}$, 77K) and d) $[Gd(\mathbf{L7})_2](CF_3SO_3)_3$ (**6**, $\lambda_{exc}$ = 41150 $cm^{-1}$, 77K). * = Rayleigh band.

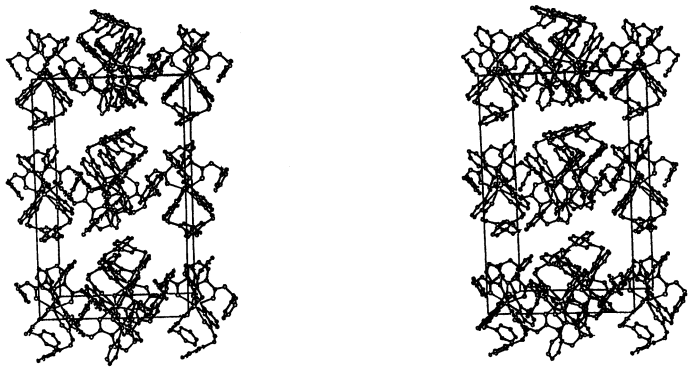

Figure S7 Stereoview of the unit cell in $[Tb(\mathbf{L8})_3]_2(CF_3SO_3)_6(CH_3CH_2CN)_3(H_2O)$ (**11**) highlighting the formation of layers parallel to the *ac* plane. Triflate anions and solvent molecules have been omitted for clarity.

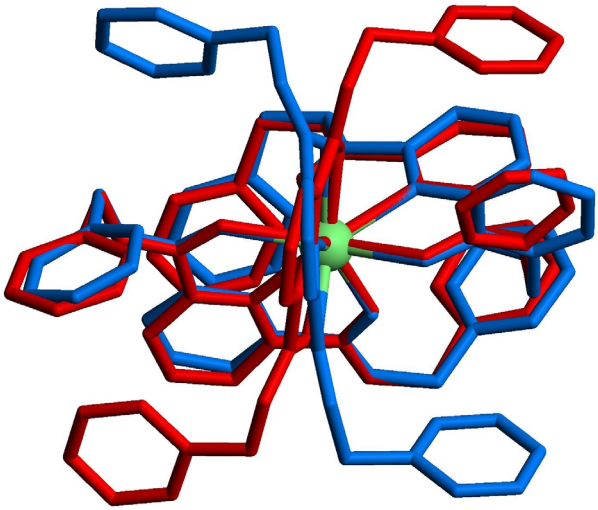

Figure S8 Superimposition of both cations of the asymmetric unit of **11** (red: **11a** ; blue: inverted structure of **11b**) showing that about 85% of the atoms are related by a pseudo centre of inversion and differ essentially by the orientations of two benzyl groups.